A Framework for Assessing Electricity Market Performance under Different Bidding Zone Configurations

(Article begins on next page)

29 June 2024

Article

A Framework for Assessing Electricity Market Performance under Different Bidding Zone Configurations

Haoke Wu [1], Tao Huang [1,*], Stefania Conti [2] and Ettore Bompard [1]

1   Department of Energy, Politecnico di Torino, 10129 Turin, Italy; haoke.wu@polito.it (H.W.);
    ettore.bompard@polito.it (E.B.)
2   Department of Electrical, Electronic and Computer Engineering, Università di Catania, 95123 Catania, Italy;
    stefania.conti@unict.it
*   Correspondence: tao.huang@polito.it

Abstract: Improper configuration of bidding zones can lead to market efficiency losses, hinder the integration of renewable energy sources (RESs), and reduce grid security. To evaluate the impact of different bidding zone configurations on market performance, we developed a multi-dimensional evaluation framework containing a series of indicators covering aspects of market efficiency, grid security, and sustainability. These indicators facilitate the comparisons among different market dispatch mechanisms. To validate the proposed framework, the reconfiguration of the Italian bidding zones has been applied to a simplified Italian grid model to compare the market performance under different bidding zone configurations. The simulation results indicate that the implemented reconfiguration has led to enhanced market efficiency and security in the Italian power system. However, the reconfiguration shows a comparatively lower reduction in greenhouse gas (GHG) emissions, suggesting a weaker sustainable performance.

Keywords: market zonal configuration; market performance assessment; market-clearing mechanisms

1. Introduction

The organization structure and pricing mechanism of the electricity market can vary between different countries and regions, but they all share the objective of promoting competition, efficiency, and security of the power systems. In the US, the electricity system is divided into several regional sub-systems managed by Regional Transmission Organizations (RTOs) or Independent System Operators (ISOs) who ensure the feasible and secure operation of the transmission grid within their respective jurisdictions [1]. The Locational Marginal Pricing (LMP) system, which matches supply with demand while considering transmission constraints, is adopted in the wholesale market. By comparison, the European electricity grid is highly interconnected with numerous cross-border transmission lines between countries, and each country has its own transmission system operator (TSO) responsible for the operation of the national transmission grid with its own dispatching and balancing mechanisms. As a result of the historical market structures and regulatory frameworks that existed within each country or region, European wholesale markets for electricity are organized in bidding zones [2]. The integration of these existing markets into larger market zones provides a practical and incremental approach to achieving market integration and cross-border trading among the participating states. Through this, a unified and efficient market where electricity can flow seamlessly across borders, market rules are harmonized, and grid operations are coordinated at the continental level can be created.

However, improperly configured bidding zones can introduce some negative impacts on different aspects. Such configurations can not only lead to inefficiencies in the electricity market but also create opportunities for market power exercise [3]. The former may result in suboptimal allocation of resources, leading to higher overall costs for electricity consumers, while the latter can drive up electricity prices and reduce competition. In regions with

significant RES, improper bidding zone configurations may hinder the integration of RES and increase pollution [4]. In addition, inadequate definitions may amplify grid congestion costs and reduce grid reliability, giving rise to bottlenecks and constraints in the transmission system [5].

Current studies have concentrated on establishing criteria for assessing market zone definitions by considering various impacts. The Capacity Allocation and Congestion Management (CACM) framework sets forth fundamental evaluation standards for delineating bidding areas. These standards encompass economic welfare, market liquidity, competition, network structure and topology, planned network reinforcement, and re-dispatch costs. However, the European Network of Transmission System Operators for Electricity (ENTSO-E) places particular emphasis on market concentration, liquidity, and price signals when evaluating the impact of zone definition on market efficiency, despite the presence of the CACM Network Code [6]. Expanding on this, [7] proposes incorporating additional criteria such as wind power flow direction, while [8] suggests considering generation costs, network security violations, and market power potential for defining bidding areas. The work in [9] introduces five indicators for assessing the effects of various bidding zone configurations in zonally priced electricity markets, including commercial exchanges evolution, price convergence, price divergence, social welfare evolution, and loop flows. Moreover, [10] outlines criteria that prioritize the applicability of the social welfare concept in bidding zone reconfiguration, including factors like congestion rent, remedial actions, differences in marginal prices, price volatility, transition costs, and social welfare. Additionally, there is a proposal to utilize sophisticated static grid models combined with dynamic market simulations to facilitate a comprehensive analysis of market efficiency, investment signals, and relevant performance indicators in evaluating bidding zone configurations [11]. Furthermore, ten key requirements have been identified in [12] for defining an effective zonal configuration based on objective and quantitative parameters. However, existing studies have failed to adequately address the comparison between zonal markets and the benchmark of nodal markets. Furthermore, they have not proposed differentiated evaluation methods for different time scales.

To address this issue, we present a multi-dimensional evaluation framework containing a series of indicators related to market efficiency, grid security, and sustainability. These indicators facilitate horizontal comparisons among key market-clearing mechanisms, including "pure economic dispatch", which is based on the intersection of supply and demand curves, without accounting for the physical network, network-constrained dispatch with nodal representation, and network-constrained dispatch with zonal representation. Our contribution is in the development of a consistent framework for the assessment of the impact of the bidding zone configuration on the market performance and designed a set of indicators for comparing the outcomes under different market mechanisms.

The remaining part of this paper is structured as follows: a multi-dimensional indicator assessment is developed in Section 2, and the case study with the simulation results is presented in Section 3. Finally, Section 4 provides some concluding remarks.

2. Designing Assessment Indicators

2.1. Fundamental Principles and Innovative Concepts

Market zone definition has an impact on both short-term [13–21] and long-term [22–25] market performance from the economics viewpoint, properly defined market zones foster stronger competition among participants, leading to more efficient resource allocation. This can mitigate congestion costs and enhance social welfare. Moreover, such zones typically allow for higher market liquidity, facilitating efficient price discovery and reducing price volatility. As far as grid security is concerned, proper zonal configuration mitigates the risk of transmission line overloads and improves the grid's resilience under contingencies. In terms of sustainability, properly defined market zones support the integration of RES and contribute to GHG emission reduction. Therefore, designing indicators to quantify these impacts is crucial. In addition, considering the existence of different market-clearing

mechanisms (for example, "pure economic dispatch" has the greatest economy, but due to network security constraints, its clearing results may not be able to run; the network-constrained dispatch with nodal representation considers both economy and security, and the clearing results can be run directly), a cross-comparison approach should be also employed for assessment.

Following the aforementioned design principles, this paper introduces indicators such as "Market efficiency", "Congestion rent", "Market liquidity" and "Price volatility" to evaluate the economic aspects, "Congestion frequency" and "Impact on security" to evaluate the grid security, and "Reduction of GHG emissions" to evaluate the sustainability. Furthermore, these indicators are designed as a tool for comparison of market-clearing outcomes under different dispatch mechanisms.

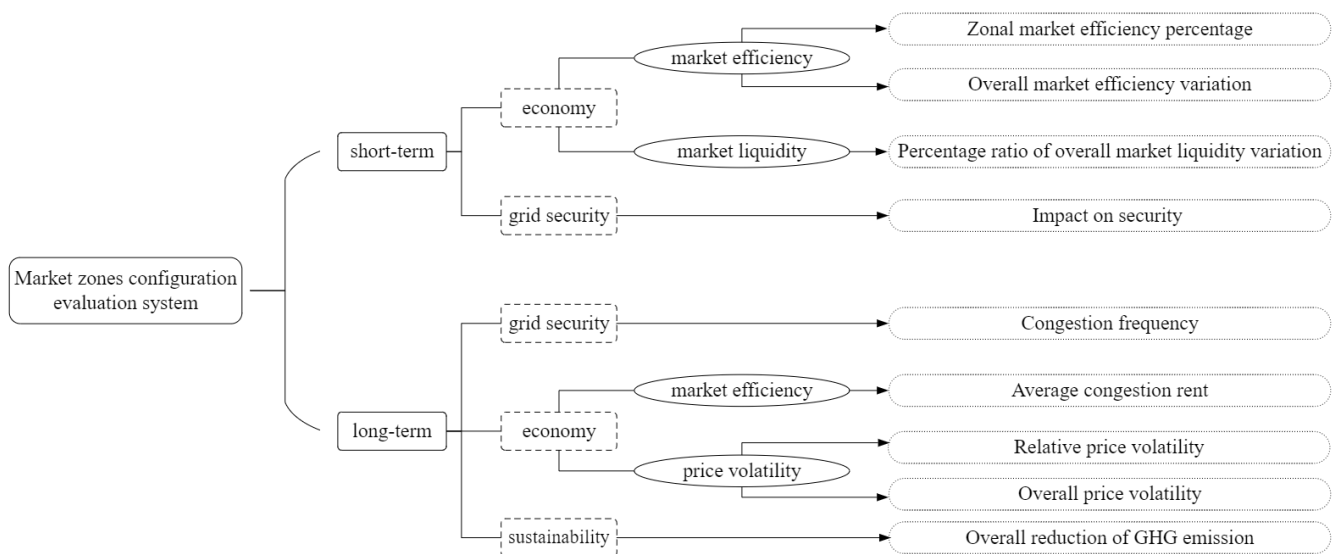The framework is shown in the Figure 1. For the specific indicators, see Section 2.3.

Figure 1. Evaluation framework for the market zones configuration.

"Market efficiency" typically is measured by the "social surplus" associated with the market transactions. This social surplus comprises three primary elements determined by the outcomes of market-clearing: "producer surplus", "consumer surplus", and "merchandise surplus". The latter becomes relevant in instances of system congestion and is also referred to as "Congestion rent" [26].

"Market liquidity" serves as a crucial indicator of competition in a market [27]. Higher market liquidity not only fosters transparency but also boosts market confidence, facilitating efficient resource allocation. In this paper, we use cleared generation quantities as a measure of market liquidity, because it mirrors the level of engagement and participation within the market.

"Price volatility" is crucial for grasping market dynamics in different market zones. Less volatility suggests more stability and predictability in electricity prices, benefiting market participants and end consumers.

"Congestion frequency" is an important indicator that provides insights into the performance of the power grid and highlights inefficiencies of the market design. Higher congestion frequency indicates that the market mechanisms are worse in effectively managing the transmission constraints.

"Impact on security" measures the influence of the market zone configuration on the surplus capacity that can be tapped into in case of unexpected events affecting the normal functioning of the power grid. A good zonal configuration should impact security as little as possible.

"Reduction of GHG emission" examines the sustainable impacts of a zonal configuration. A properly designed zonal configuration should aim to reduce carbon emissions and promote the integration of RES.

2.2. Market-Clearing Model

The market dispatch process operates on microeconomic principles and hinges on the competition among market participants. It aims to utilize this competition to maximize social surplus [28]. Various market surpluses can be calculated as follows.

Producer surplus is the monetary gain obtained by producers in the market due to the fact that the market-clearing price is higher than the price at which they are willing to sell [29].

$$s_r^G = \int_0^{p_r^{G*}} \left(\lambda p_r^{G*} - v_r^G \left(p_r^G \right) \right) dp_r^G \tag{1}$$

where λ is the market-clearing price, p_r^G and $v_r^G(p_r^G)$ are the cleared generation and the stepwise offer function of generation unit r, respectively. In this paper, * refers to the values at market equilibrium.

Consumer surplus is the monetary gain obtained by consumers in the market due to the market-clearing price being lower than the price at which they are willing to buy [29].

$$s_s^D = \int_0^{p_s^{D*}} \left(v_s^D \left(p_s^D \right) - \lambda p_s^{D*} \right) dp_s^D \tag{2}$$

where p_s^D and $v_s^D(p_s^D)$ are the cleared demand and the stepwise bid function of load unit s, respectively.

In case of congestion, the market-clearing price fluctuates depending on the precise locations of power injections and withdrawals across the network. This gives rise to merchandise surplus, which can also be conceptualized as congestion rent [30].

$$s^M = \sum_{i=1}^B p_i \lambda_i \tag{3}$$

where B is the set of buses, and p_i and λ_i are, respectively, the net injection power and the clearing price of bus i.

The social surplus can be calculated as the sum of the quantities calculated in (1)–(3).

$$s^S = s_r^G + s_s^D + s^M \tag{4}$$

2.2.1. Pure Economic Dispatch

By lumping the electricity network into a single node, all constraints linked with the network are neglected. In this scenario, the market dispatch process only hinges on economic factors to facilitate electricity exchange between generators and loads [28]. Mathematically, the market dispatch at time t can be expressed as follows:

$$\min - \hat{S}^{S,t} \left(\underline{\hat{p}}^{G,t}, \underline{\hat{p}}^{D,t} \right) \tag{5}$$

$$\text{s.t.} \sum_{r=1}^G \underline{\hat{p}}^{G,t} - \sum_{s=1}^D \underline{\hat{p}}^{D,t} = 0 \tag{6}$$

$$\underline{p}^{Gmn} \leq \underline{\hat{p}}^{G,t} \leq \underline{p}^{Gmx} \tag{7}$$

$$\underline{p}^{Dmn} \leq \underline{\hat{p}}^{D,t} \leq \underline{p}^{Dmx} \tag{8}$$

where $\hat{S}^{S,t}$, $\underline{\hat{p}}^{G,t}$, and $\underline{\hat{p}}^{D,t}$ are, respectively, the social surplus and the vectors of power injection and withdrawal, (6)–(8) are the power balance, the generation output limits, and the demand limits, respectively.

2.2.2. Network-Constrained Dispatch with Nodal Representation

By considering the market clearing with the one-step approach, which integrates pure market dispatch with network constraints [3], the model at a specific time t can be formulated as follows:

$$\min - S^{S,t}\left(\underline{p}^{G,t}, \underline{p}^{D,t}\right) \tag{9}$$

$$\text{s.t. } \underline{p}^t = B\delta^t \tag{10}$$

$$\underline{p}^t = \Omega \underline{p}^{G,t} - \Psi \underline{p}^{D,t} \tag{11}$$

$$\underline{f}^t = H\delta^t \tag{12}$$

$$\underline{f}^t \begin{cases} > 0 \rightarrow \underline{f}^t < \underline{f}^+ \\ < 0 \rightarrow -\underline{f}^t < \underline{f}^- \end{cases} \tag{13}$$

$$\underline{p}^{Gmn} \leq \underline{p}^{G,t} \leq \underline{p}^{Gmx} \tag{14}$$

$$\underline{p}^{Dmn} \leq \underline{p}^{D,t} \leq \underline{p}^{Dmx} \tag{15}$$

$$\underline{\delta}^{mn} \leq \underline{\delta}^t \leq \underline{\delta}^{mx} \tag{16}$$

where $S^{S,t}$, $\underline{p}^{G,t}$, and $\underline{p}^{D,t}$ are, respectively, the social surplus and the vectors of power injection and withdrawal with nodal network constraints; B is the admittance matrix for the network; δ is the vector of bus voltage angles; H is the transmission matrix; Ω and Ψ are, respectively, the connection matrices for generators and loads; finally, expressions (13)–(16) are, respectively, the limits of transmission, generation output, demand, and bus voltage angle.

2.2.3. Network-Constrained Dispatch with Zonal Representation

(A)   Interzonal dispatch

For a given market configuration c, at time t, the interzonal dispatch [31,32] can be formulated as follows:

$$\min - S^{S,t,c,0}\left(\underline{p}^{G,t,c,0}, \underline{p}^{D,t,c,0}\right) \tag{17}$$

$$\text{s.t. } \underline{p}^{Z,t,c,0} = \widetilde{B}\widetilde{\delta}^{t,c,0} \tag{18}$$

$$\underline{p}^{Z,t,c,0} = \widetilde{\Omega}\Omega \underline{p}^{G,t,c,0} - \widetilde{\Psi}\Psi \underline{p}^{D,t,c,0} \tag{19}$$

$$\underline{f}^{I,t,c,0} = \widetilde{H}\widetilde{\delta}^{t,c,0} \tag{20}$$

$$\underline{f}^{I,t,c,0} \begin{cases} > 0 \rightarrow \underline{f}^{I,t,c,0} < \underline{f}^{I+} \\ < 0 \rightarrow -\underline{f}^{I,t,c,0} < \underline{f}^{I-} \end{cases} \tag{21}$$

$$\underline{p}^{Gmn} \leq \underline{p}^{G,t,c,0} \leq \underline{p}^{Gmx} \tag{22}$$

$$\underline{p}^{Dmn} \leq \underline{p}^{D,t,c,0} \leq \underline{p}^{Dmx} \tag{23}$$

$$\widetilde{\underline{\delta}}^{mn} \leq \widetilde{\underline{\delta}}^{t,c,0} \leq \widetilde{\underline{\delta}}^{mx} \tag{24}$$

where $S^{S,t,c,0}$, $\underline{p}^{G,t,c,0}$, and $\underline{p}^{D,t,c,0}$ are, respectively, the social surplus and the vectors of power injection and withdrawal with zonal constraints; (19) represents the power balance, (20) the line flows; (21)–(24) are the expressions of the zonal limits of transmission, generation output, demand, and bus voltage angle, respectively. In this paper, the symbol $\widetilde{\cdot}$ denotes a value for the zonal model.

(B)   Intrazonal dispatch

In case of intrazonal congestion, a redispatch inside the congested zone is needed. The redispatch problem can be formulated as follows:

$$
\min_{\substack{b^{MG}(r) = z \\ b_s^{MD}(s) = z}} \sum_{s=1}^{D} \underline{\Delta p}_s^{D,t,c} \cdot v_s^{D'} - \sum_{r=1}^{G} \underline{\Delta p}_r^{G,t,c} \cdot v_r^{G'} \tag{25}
$$

$$
\text{s.t. } \underline{p}^{z,t,c} = B^z \delta^{z,t,c} \tag{26}
$$

$$
\underline{p}^{z,t,c} = \Omega^z \left(\underline{p}_r^{G,t,c,0} + \underline{\Delta p}_r^{G,t,c} \right) - \Psi^z \left(\underline{p}_s^{D,t,c,0} + \underline{\Delta p}_s^{D,t,c} \right) \tag{27}
$$

$$
\underline{f}^{z,t,c} = H^z (B^z)^{-1} \underline{p}^{z,t,c} \tag{28}
$$

$$
\underline{f}^{z,t,c} \begin{cases} > 0 \rightarrow \underline{f}^{z,t,c} < \underline{f}^{z+} \\ < 0 \rightarrow -\underline{f}^{z,t,c} < \underline{f}^{z-} \end{cases} \tag{29}
$$

$$
\underline{p}_r^{Gmn} - \underline{p}_r^{G,t,c,0} \leq \underline{\Delta p}_r^{G,t,c} \leq \underline{p}_r^{Gmx} - \underline{p}_r^{G,t,c,0} \tag{30}
$$

$$
\underline{p}_s^{Dmn} - \underline{p}_s^{D,t,c,0} \leq \underline{\Delta p}_s^{D,t,c} \leq \underline{p}_s^{Dmx} - \underline{p}_s^{D,t,c,0} \tag{31}
$$

where $\underline{\Delta p}_r^{G,t,c}$ is the vector of adjustment offer power of generation units, $\underline{\Delta p}_s^{D,t,c}$ is the vector of adjustment bid power of load units, and $v_r^{G'}$ and $v_s^{D'}$ are, respectively, the corresponding adjustment price of offer and bid. Expressions (26)–(31) represent constraints similar to that of the interzonal dispatch. Here, the symbol $\cdot^z$ indexes the zones.

2.3. Representation of the Indicators
2.3.1. Short-Term Indicators

- Zonal market efficiency percentage

The zonal market efficiency of the zone configuration c, at time t, can be assessed by comparing the interzonal dispatch and the benchmark of the pure economic dispatch in terms of the social surplus.

$$
\hat{\xi}_e^{t,c,0} = \frac{S^{S,t,c,0}}{\hat{S}^{S,t}} \times 100\% \tag{32}
$$

- Overall market efficiency variation

The overall market efficiency variation is the percent value of the decrease in the social surpluses of the network-constrained dispatch with the zonal representation related to that of the network-constrained dispatch with nodal representation.

$$
\xi_e^{c,t} = \frac{s^{S,t} - \tilde{s}^{S,t,c}}{s^{S,t}} \times 100\% \tag{33}
$$

where $\tilde{s}^{S,t,c}$ is the social surplus in network-constrained dispatch with zonal representation.

- Percentage ratio of overall market liquidity variation

The percent ratio of overall market liquidity variation can be expressed as the percent variation in the cleared generation quantity in the network-constrained dispatch with zonal representation with respect to that of the network-constrained dispatch with nodal representation.

$$
\xi_l^{t,c} = \frac{\sum_{b=1}^{B} \Omega \underline{p}^{G,t*} - \sum_{z=1}^{Z} \overset{\sim}{\Omega} \Omega^z \underline{p}_r^{G,t,c}}{\sum_{b=1}^{B} \Omega \underline{p}^{G,t*}} \times 100\% \tag{34}
$$

where $\underline{p}_r^{G,t,c}$ is the cleared generation quantity of the network-constrained dispatch with zonal representation.

- Impact on security

The impact on security can be determined by the changes in the available system spinning reserves, including both the upward and downward reserves, in the network-constrained dispatch with zonal representation.

$$\overset{\sim t,c}{\zeta}_{sm} = \left| \sum_{z=1}^{Z} \sum_{g=1}^{G^z} \Delta p_r^{G,t,c} \right| \tag{35}$$

where $\Delta p_r^{G,t,c}$ is the cleared generation quantity in the intrazonal dispatch during the time t.

2.3.2. Long-Term Indicators

- Congestion frequency

Congestion frequency over the considered time period t can be calculated as follows:

$$c_f^{c,0} = \frac{\sum_{t=1}^{T} E^{t,c,0}}{T \times NL} \times 100\% \tag{36}$$

where $E^{t,c,0}$ is the number of congestion events under zone configuration c at time t, while NL is the total number of transmission lines of the network.

- Average congestion rent

Congestion can result in market inefficiency. The average weighted congestion rent under the zonal configuration over the considered period T can be expressed as follows:

$$\overset{\sim c,0}{c} = \frac{1}{T} \sum_{t=1}^{T} \underline{p}^{Z,t,c,0} \overset{\sim t,c,0}{\underline{\lambda}} \tag{37}$$

where $\overset{\sim t,c,0}{\underline{\lambda}}$ is the price differential between two zones under zone configuration c at the time t.

- Overall reduction in GHG emissions

Generators whose energy carriers are gas, oil, coal, and biomass can cause GHGs (mainly CO_2, N_2O, and CH_4). Given a set $\mathcal{R} = \{$Gas, Oil, Coal, Biomass$\}$ of GHG energy, using r as the indicator, and a set $\mathcal{E} = \{CO_2, N_2O, CH_4\}$ of GHGs, use e as the indicator. To evaluate the sustainable impacts of the zone configuration, we measure the difference in GHG emissions between the network-constrained dispatch with zonal representation and the network-constrained dispatch with nodal representation throughout the considered period T.

$$\overset{\sim c,0}{\zeta}_{GR} = \sum_{t=1}^{T} \sum_{e \in E} \rho_e^r \left(\sum^{r \in R} p_r^{G,t*} - \sum^{r \in R} p_r^{G,t,c*} \right) \tag{38}$$

where $\sum^{r \in R} p_r^{G,t*}$ and $\sum^{r \in R} p_r^{G,t,c*}$ are, respectively, the total r-type generation of the network-constrained dispatch with nodal representation and the network-constrained dispatch with zonal representation under configuration c; at the time t, ρ_e^r denotes the quantity of gas e that can be produced by one unit of r-type generation. The values of ρ_e^r are given in [33].

- Relative price volatility

By employing the pure economic dispatch as the benchmark, we can measure and quantify the relative price volatility associated with a specific zonal configuration c throughout the considered period T.

$$\hat{\varsigma}_{pv}^{c,0} = \sqrt{\frac{1}{T-1} \sum_{t=1}^{T} \left(\ln \left(\frac{\overset{\sim t,c,0}{\lambda}}{\hat{\lambda}_{av}^t} \right) - \frac{1}{T} \sum_{t=1}^{T} \ln \left(\frac{\overset{\sim t,c,0}{\lambda}}{\hat{\lambda}_{av}^t} \right) \right)^2} \tag{39}$$

where $\overset{\sim t,c,0}{\lambda}_{av}$ and $\hat{\lambda}^t_{av}$ are, respectively, the average weighted price of the interzonal dispatch and the pure economic dispatch at the time t.

- Overall price volatility

By employing the network-constrained dispatch with nodal representation as the benchmark, we can quantify the overall price volatility associated with a specific zonal configuration c throughout the considered period T.

$$\xi^c_{pv} = \sqrt{\frac{1}{T-1}\sum_{t=1}^{T}\left(\ln\left(\frac{\overset{\sim t,c,0}{\lambda}_{av} + \lambda^{t,c}_{av}}{\lambda^t_{av}}\right) - \frac{1}{T}\sum_{t=1}^{T}\ln\left(\frac{\overset{\sim t,c,0}{\lambda}_{av} + \lambda^{t,c}_{av}}{\lambda^t_{av}}\right)\right)^2} \qquad (40)$$

where $\lambda^{t,c}_{av}$ and λ^t_{av} are, respectively, the average weighted price of the intrazonal dispatch and the network-constrained dispatch with nodal representation at the time t.

3. Case Study

3.1. Simulation Settings

In this section, we present a comparative analysis in terms of market performance between the two Italian bidding zone configurations existing in 2020 and 2021, by using the developed indicators.

3.1.1. Network

The Italian transmission network is a part of the synchronous European grid managed by ENTSO-E that coordinates the various national TSOs. It has interconnections with neighboring countries such as France, Switzerland, Slovenia, and Austria, facilitating cross-border energy trading. Operated and managed by Terna S.p.A., mandated to ensure secure and reliable electricity transmission across the country, the grid comprises an extensive infrastructure of high voltage power lines, substations, transformers, and associated equipment. These components form a network that connects power generators, including conventional and RES power plants, to transmission and distribution networks, as well as directly to major consumption centers. In 2022, the total installed capacity in Italy was 118.4 GW, with the RES plants accounting for 49.6% [34].

Modelling generation and demand in the Italian grid involves investigating the distribution of loads and natural resources (e.g., solar, wind, and hydroelectric). For instance, the Northern regions have larger hydroelectric production due to the proximity to the Alps. A proper modelling of the transmission network is crucial for our evaluation. Detailed network models with many physical parameters and accurate topology representation are cumbersome to handle, while, on the other hand, oversimplified models often neglect fundamental correlations and structures of the real systems, thus introducing the risk of non-accurate results. Then, in this research, we extracted a 339-bus Italian network from the PyPSA-Eur model dataset (see Figure 2), which is realized by a Python 3.10.6—based multi-energy modelling software package.

3.1.2. Market

The Italian Power Exchange (IPEX) comprises a spot market (MPE), a forward market (MTE), and a platform facilitating the physical delivery of contracts from the financial derivatives segment of the Italian Stock Exchange (CDE). Within the spot market, there are four sub-markets: day-ahead (MGP), intra-day (MI), daily products (MPEG), and ancillary services (MSD) markets [35]. The GME (Italian acronym for "Gestore dei Mercati Energetici"), acting as the central market operator, oversees IPEX, particularly managing forward electricity contracts concluded over the power exchange. In the day-ahead market, transactions take place between the ninth day preceding physical delivery and the day before delivery. Sellers submit hourly offers for each generating unit, specifying both the quantity and the minimum price for trading power. The supply curve is constructed by

organizing offers in ascending order of price, while the demand curve is shaped by ordering bids in descending price order. Participants can submit a maximum of 24 bids/offers daily, falling into three categories: simple (indicating volume and price), multiple (dividing overall volume for the same hour), or pre-defined (daily submissions to GME). The hourly market price is established through a uniform auction mechanism as the intersection of the demand and supply curves, with accepted units receiving, uniformly, the market-clearing price. If the interzonal market constraints are not binding, the market clearing leads to a unique market-clearing price, while when they are binding, the market is split into zones with different zonal prices.

Figure 2. 339-bus simplified Italian transmission network (179 lines at 220 kV and 233 lines at 380 kV).

Producers receive zonal prices during congestion, while buyers still pay a National Single Price (PUN), an average of the zonal prices weighted on the traded quantity.

In Italy, until 31 December 2020, there were six market bidding zones: North, Centre-North, Centre-South, South, Sicily, and Sardinia. Since 2021 on, the current zonal configuration includes seven zones: North, Centre-North, Centre-South, South, Sicily, Calabria, and Sardinia (Figure 3). This change was primarily driven by the need to adapt to the changing energy scenario, enhance market efficiency, and optimize grid management considering evolving generation patterns and regional dynamics.
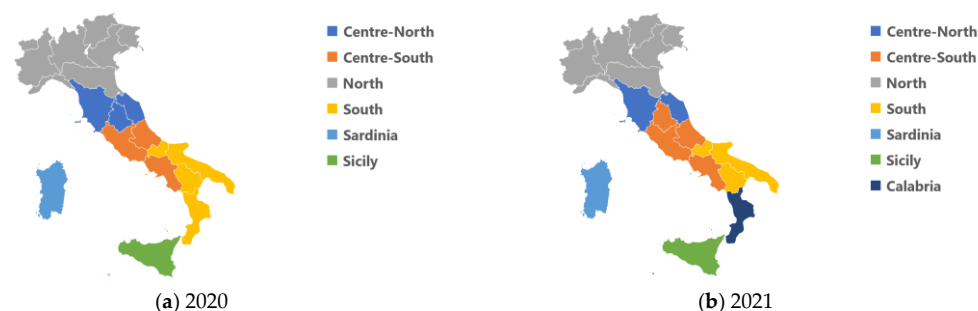

Figure 3. Italian bidding zones configuration in 2020 (**a**) and since 2021 (**b**).

Previously there were four production hubs (Priolo, Foggia, Brindisi, and Rossano) in which the generation capacity was higher than the transport capacity of the connecting lines, while now this issue has been solved by the enhancement of the transmission infrastructure.

Then, the decommissioning of some thermal generation was necessary to align with the evolving energy scenario of large penetration of RESs.

Moreover, the introduction of a new bidding zone, "Calabria," was in response to the growing relevance of renewable generation in that region. Establishing Calabria as a separate bidding zone allowed for more precise pricing. Additionally, the reallocation of the Umbria region from the Centre-North to the Centre-South zone was intended to better capture the impact of the regional market on the grid congestion. This intervention ensured

the zonal configuration alignment with the geographical distribution and operational dynamics of the electricity market [36].

3.1.3. Data

Given the potential for strategic bidding across different zonal markets (or the reaction of each generation plant in terms of costs to the reconfigured bidding zones), the unavailability of the real network flow information, as well as the lack of knowledge on loads distribution, we cannot use the GME data as inputs for our simulation. Therefore, besides using the simplified Italian transmission grid model introduced in Section 3.1.1, we use the following data for the costs of generators and demand:

(1) To determine the hourly electricity input of each generator and load, we used the approach outlined in [37], since this methodology ensures a more accurate reflection of generator costs and improves the reliability of our analysis;

(2) This research does not consider strategic bidding, to maintain focus on the main objective, the bidding prices for loads in each period are uniformly set to 300€/MWh, and all generators bid their true marginal costs.

3.2. Simulation Results and Discussion

We performed 8760 h of simulation for the years 2020 and 2021. By using the network, market, and data described in Section 3.1 in different market models in Section 2.2, the corresponding clearing results for pure economic dispatch, network-constrained dispatch with nodal representation, and network-constrained dispatch with zonal representation can be obtained. After that, the market-clearing results are fed into the indicators formulated in Section 2.3.

After completing the simulation, we first verified the validity of the market results. The developed simplified model has been compared in terms of generation dispatch from different sources with real market dispatch, in 2020 and 2021, provided by Terna [38]. The difference between the two is in the range of [−0.6%, 1.2%], and this validates the methodology we used to set up the input for market analysis (Figure 4a,b).
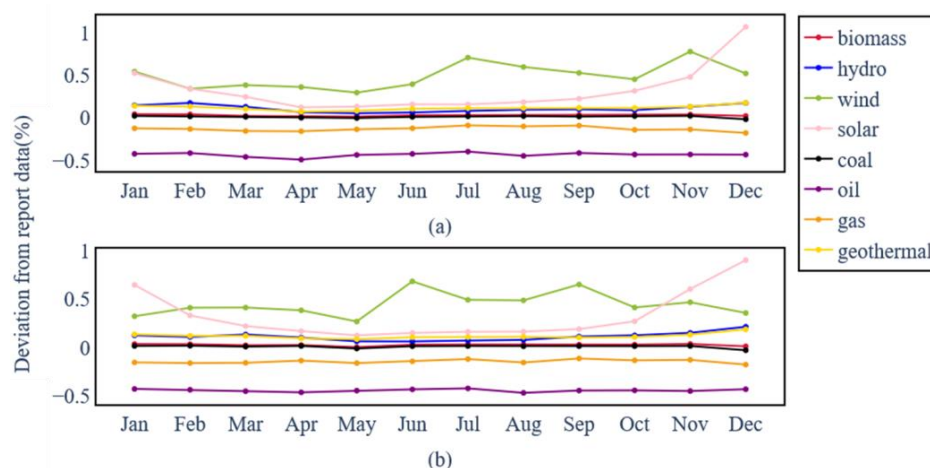

Figure 4. Simulation results vs. market outcomes (2020 (**a**) and 2021 (**b**)).

Next, to provide an intuitive reflection of the impact of the Italian bidding zone reconfiguration at a fundamental level, Figure 5 provides a comparative analysis of the average social surplus under the two zonal configurations (histogram), while the lines present a comparison in terms of price convergence. With respect to the year 2020, the overall market exhibits increased social surplus throughout 2021, with the latter overcoming the former in terms of social surplus in all months, except in July. In particular, February recorded the highest average social surplus at 3.32 B€/h, which is a 25.28% year-over-year

(YoY) increase from 2020, while April recorded the lowest value at 2.6 B€/h, reflecting a 16.6% YoY increase concerning the previous year.
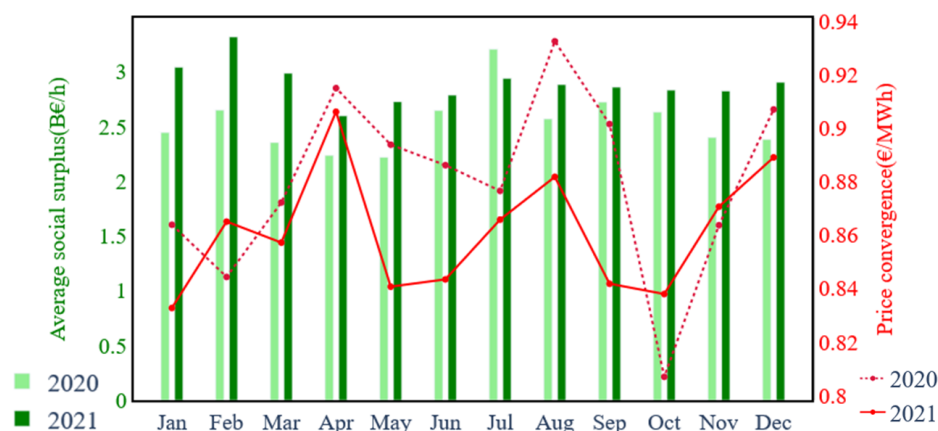

Figure 5. Comparison of average social surplus and price convergence for 2020/2021 configuration.

Price convergence is calculated as the root mean square of the price differences with respect to the weighted average price; considering the 2021 configuration, the price convergence generally registers lower values compared to that of the 2020 configuration, with exceptions in February, October, and November. This indicates that the 2021 configuration has more consistency and uniformity in prices.

The plots in Figure 6 present a comparison between the short-term indices, calculated with reference to the two zonal configurations in 2020 and 2021. Notably, the market efficiency obtained in 2021 tends to overcome that of 2020 (Figure 6a). The values for the maximum, upper quartile, median, mean, lower quartile, and minimum in 2021 show, respectively, increases of 4.59%, 1.72%, 5.86%, 7.83%, 9.87%, and 9% with respect to the values in 2020. This indicates that 2021 shows a more effective allocation and utilization of energy resources within the interzonal dispatch, since reconfiguration changes the different types of units that win the bid under the same bidding strategy, thus affecting the market price and the social surplus. Considering the intrazonal dispatch, it becomes apparent that the overall market efficiency variation in 2020 exceeds that in 2021 (Figure 6b). Specifically, the median and mean values of the former are 2.14% and 4.35%, higher than the values of the latter, respectively. This indicates that the social surplus of the network-constrained dispatch with zonal representation in 2021 shows a smaller difference compared to the network-constrained dispatch with nodal representation. Moving on to Figure 6c, the percentage ratio of the overall market liquidity of 2021 is higher than that of 2020, and the mean value of 2021 (−0.34%) is higher than that of 2020 (−0.52%). As for the impact on security, a general lower trend was observed in 2021 (Figure 6d). The values for the maximum, mean, and minimum in 2021 exhibit a decrease of 23.17%, 12.42%, and 22.7%, respectively, with respect to the values in 2020.

To explore the factors that affect the first long-term indicator (congestion frequency), we considered the correlation between congestion frequency and variables including load, period, and generation of a specific type. No significant correlation was found among them. Here, we single out the most relevant factor. Figure 7 focuses on the impacts of annual non-RES generation on congestion frequency. The bar chart presents the annual non-RES generation, whereas the line chart depicts the annual congestion frequency that falls within the range from 0% to 15%, aligning consistently with findings from prior research on Italian bidding zones [39]. This alignment is useful to further validate the adopted approach. Based on the interzonal flows, the zones can be divided into two states: exporting power and importing power. In both configurations, Sardinia, Sicily, and Centre-North are net importers, although the geographical scope of the Centre-North changed in 2021 (see Figure 3). Sardinia experienced negligible congestion with a frequency close to 0% in both years. However, the reconfiguration led to a slight rise in Sicily's congestion frequency,

increasing from 0.04% to 0.11%. In the North zone, where the geographical scope remains unchanged, congestion frequency decreased from 1.73% in 2020 to just 0.01% in 2021. The interconnections between the two zones of Calabria and the South, which originated by splitting the previous original South zone, show congestion frequencies of 14.54% and 7.11% in 2021, respectively. Both values are higher than the 2020 congestion frequency of the South zone, which was 5.52%. This has to do with the elimination of the four production hubs as well. In addition, a higher power supply from non-RES generation increases the congestion frequency in importing regions, while the opposite effect occurs when non-RES production is present in exporting regions, as can be seen in Figure 7c,d.
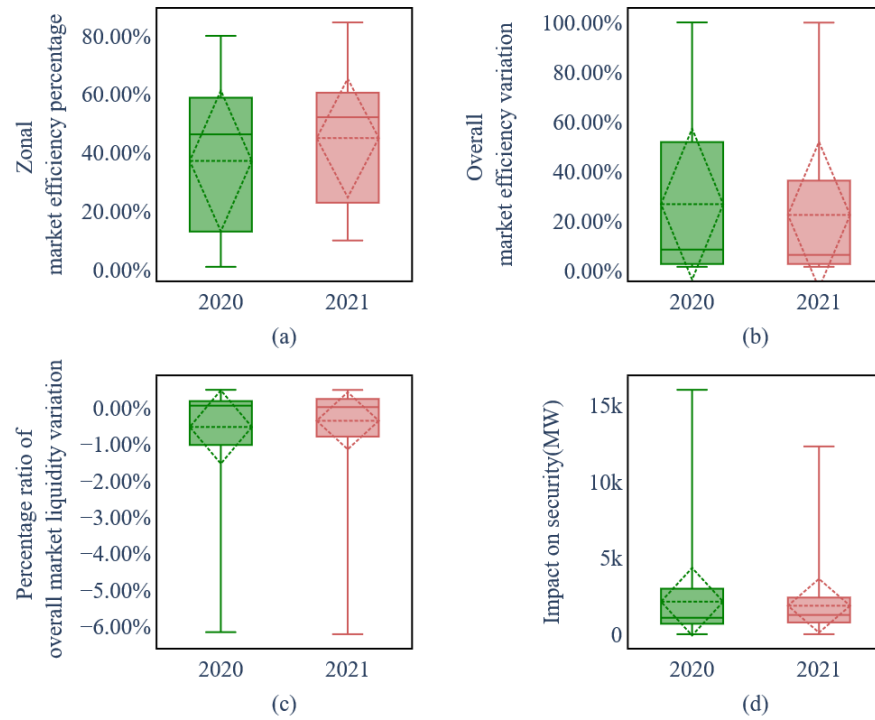

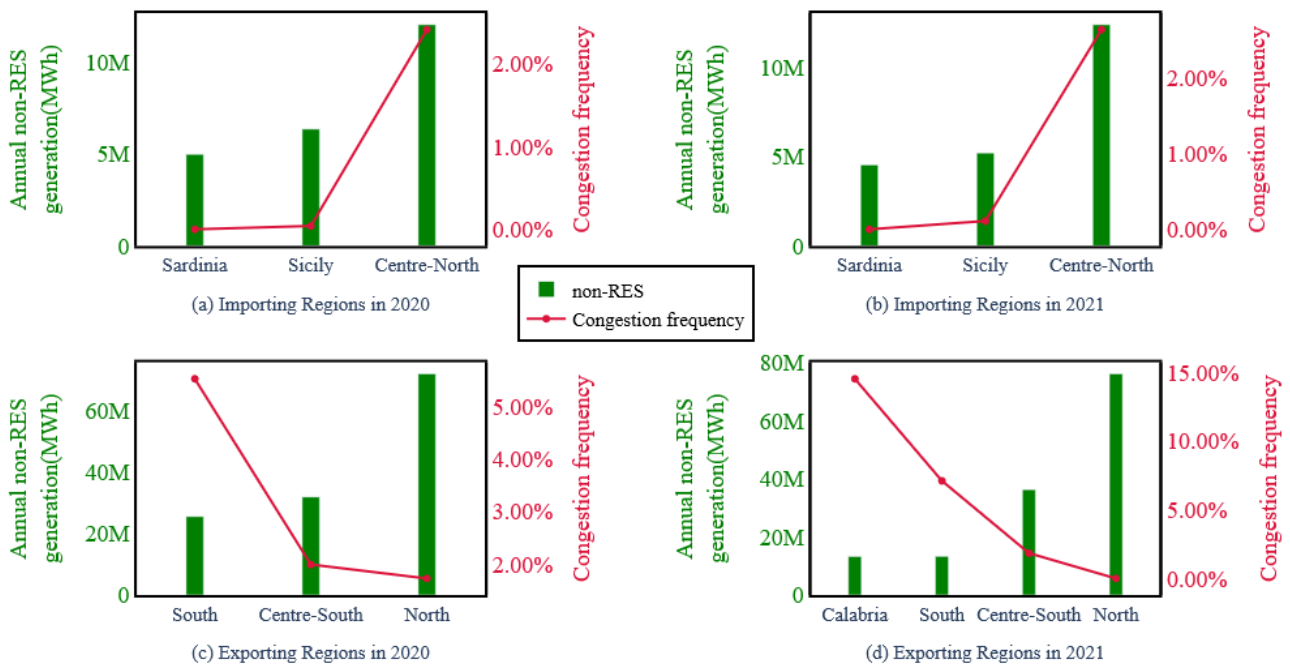**Figure 6.** Comparison of short-term indicators in 2020 and 2021.

Figure 7. Annual non-RES generation and congestion frequency.

Figure 8 illustrates the seasonal values of the remaining four long-term indicators for the years 2020 and 2021. We considered the astronomical definition of seasons (spring equinox, summer solstice, fall equinox, and winter solstice). The average congestion rent is lower under the 2021 configuration compared to that of 2020 across all seasons. The most significant difference occurs during winter (8.25 k€/h), followed by summer (6.86 k€/h), with the smallest difference observed in spring (1.17 k€/h) (Figure 8a). Despite the overall reduction in GHG emissions for both configurations being negative, showing an increase with respect to the network-constrained dispatch with nodal representation, the 2021 performance is notably lower, particularly during the spring, with a 10% YoY increase from 2020 (Figure 8b). When only considering interzonal dispatch, the relative price volatility remains almost identical under both configurations, except for marginal differences in spring and summer where 2020 registers a negligible uptick with respect to 2021 (Figure 8c). In the context of intrazonal dispatch, the overall price volatility in 2020 exceeds that of 2021 across all four seasons, with differences ranging from 0.1€/h to 0.16€/h. This implies that the electricity prices under the 2021 configuration exhibit greater stability and predictability (Figure 8d).
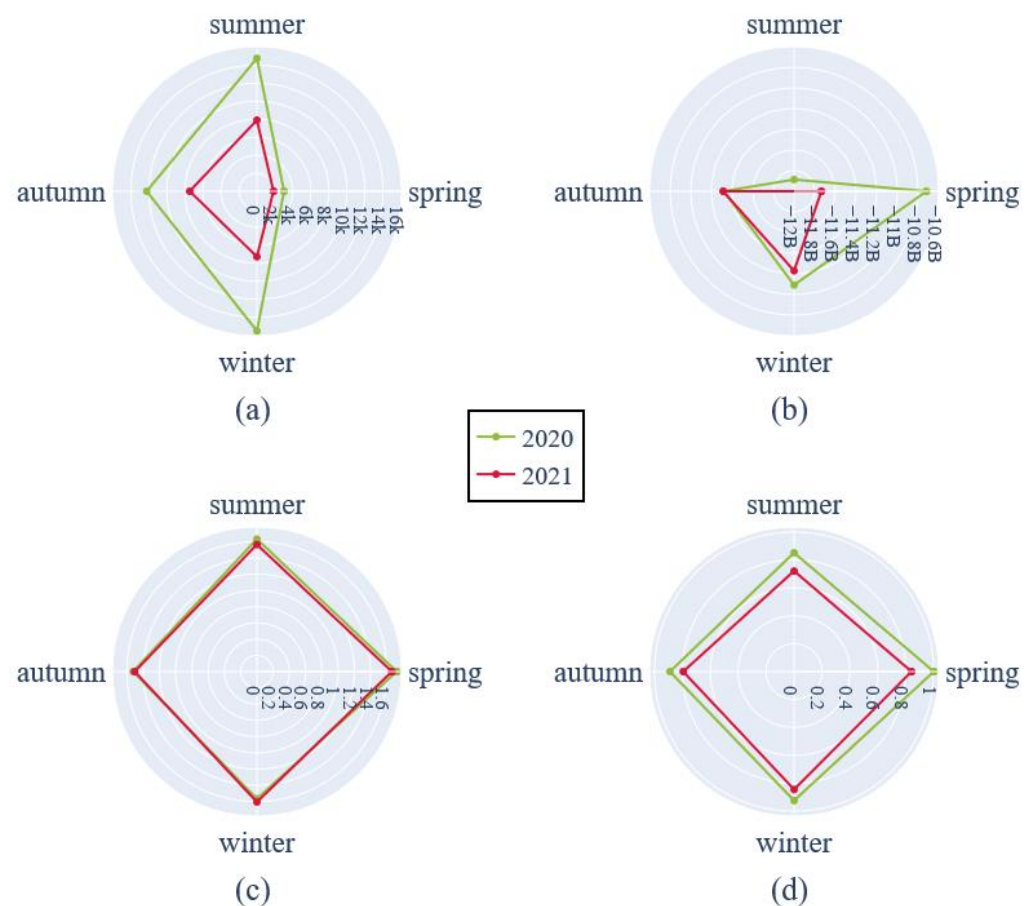

Figure 8. (**a**) Average congestion rent (€/h); (**b**) Overall reduction in GHG emissions (t); (**c**) Relative price volatility (€/h); (**d**) Overall price volatility (€/h).

4. Conclusions

The proposed methodology, based on a series of performance indicators for electricity market assessment under different configurations of the bidding zones, proved to be general enough for networks of various sizes, provided that sufficient information is available on RES and load distribution, on the geographic location of each bus, and the line parameters.

The simulation results show that the 2021 configuration has yielded positive outcomes, with increased social surplus and reduced price convergence. Irrespective of whether

intrazonal dispatch is taken into consideration, the 2021 configuration demonstrates a closer alignment of social efficiency with the corresponding benchmark comparison with respect to 2020. This suggests that the reconfiguration achieves a more effective allocation and utilization of energy resources. The mean value of the percentage ratio of overall market liquidity variation in 2021 (-0.34%) overcomes that of 2020 (-0.52%), indicating improved competitiveness and transparency in 2021. The mean value for the impact on security in 2021 exhibits a decrease of 12.42% with respect to 2020, showing that the 2021 configuration has a better performance on grid security.

Concerning the long-term performance, 2021 achieves less congestion rent in all seasons. The zonal reconfiguration results in an almost complete elimination of congestion frequency in the North zone. However, it indicates the need for grid reinforcement in the southern region to manage the rise in congestion frequency. Furthermore, given the direct proportionality between non-RES production and congestion frequency in the importing region, and the inverse proportionality in the exporting region, our findings strongly advocate prioritizing the installation of non-RES in exporting regions to address congestion-related challenges, offering valuable policy recommendations. Through a comprehensive analysis of relative price volatility and overall price volatility, it becomes evident that the electricity price under the 2021 zonal configuration is more stable, consistent, and predictable, delivering benefits to both market participants and end-users. However, the 2021 configuration exhibits a smaller overall reduction in GHG emissions compared to the 2020 configuration, potentially indicating a less favorable performance in terms of sustainability, particularly evident during the spring with a 10% year-over-year increase from 2020.

These findings provide valuable insights for evaluating the zonal configuration and highlight opportunities for its enhancement. The strategic bidding behavior of market participants, which can influence dispatch results, has not been considered. Additionally, this paper does not explore the utilization of these assessment indicators to determine an optimal configuration (to maximize market efficiency, promote renewable energy integration, minimize reliance on fossil fuels, etc.). Therefore, further research is necessary to address these issues and provide a more comprehensive understanding of the topic.

Author Contributions: Conceptualization, T.H. and E.B.; Methodology, H.W., T.H. and S.C.; Software, H.W.; Validation, H.W., S.C. and E.B.; Investigation, S.C.; Writing—original draft, H.W. and T.H.; Writing—review & editing, H.W., T.H., S.C. and E.B.; Supervision, T.H.; Project administration, E.B. All authors have read and agreed to the published version of the manuscript.

Data Availability Statement: The original contributions presented in the study are included in the article, further inquiries can be directed to the corresponding authors.

Conflicts of Interest: The authors declare no conflicts of interest.

References

1. Ela, E.; Milligan, M.; Bloom, A.; Townsend, A.; Levin, T. *Evolution of Wholesale Electricity Market Design with Increasing Levels of Renewable Generation*; Hirth, L., Schlecht, I., Eds.; Market-Based Redispatch in Zonal Electricity Markets; Social Science Electronic Publishing: Rochester, NY, USA, 2014.
2. Hirth, L.; Schlecht, I. Market-Based Redispatch in Zonal Electricity Markets: The Preconditions for and Consequence of Inc-Dec Gaming. 2020. Available online: https://hdl.handle.net/10419/222925 (accessed on 1 November 2023).
3. Bompard, E.; Huang, T.; Lu, W. Market power analysis in the oligopoly electricity markets under network constraints. *IET Gener. Transm. Distrib.* **2010**, *4*, 244–256. [CrossRef]
4. Wu, Y.; Liang, X.; Huang, T.; Lin, Z.; Li, Z.; Hossain, M.F. A hierarchical framework for renewable energy sources consumption promotion among microgrids through two-layer electricity prices. *Renew. Sustain. Energy Rev.* **2021**, *145*, 111140. [CrossRef]
5. Huang, T.; Bompard, E.; Yan, Z. Congestion management impacts on bilateral electricity markets under strategic negotiation. *Electr. Power Syst. Res.* **2011**, *81*, 1161–1170. [CrossRef]
6. Dusolt, A. NETWORK CODES: THE RULES OF THE GAME OF THE ENERGY TRANSITION. *Eur. Energy Clim. J. (Claeys Casteels BV)* **2020**, *9*, 29. [CrossRef]

7. Supponen, M. Influence of National and Company Interests on European Electricity Transmission Investments. Doctoral Dissertation, Aalto University, Espoo, UK, 2011.

8. Breuer, C.; Moser, A. Optimized bidding area delimitations and their impact on electricity markets and congestion management. In Proceedings of the 11th International Conference on the European Energy Market (EEM14), Krakow, Poland, 28–30 May 2014; pp. 1–5.

9. Sarfati, M.; Hesamzadeh, M.R.; Canon, A. Five indicators for assessing bidding area configurations in zonally-priced power markets. In Proceedings of the 2015 IEEE Power & Energy Society General Meeting, Denver, CO, USA, 26–30 July 2015; pp. 1–5.

10. Bemš, J.; Králík, T.; Knápek, J.; Kradeckaia, A. Bidding zones reconfiguration—Current issues literature review, criterions and social welfare. In Proceedings of the 2016 2nd International Conference on Intelligent Green Building and Smart Grid (IGBSG), Prague, Czech Republic, 27–29 June 2016; pp. 1–6.

11. Brouhard, T.; Hennebel, M.; Petit, M.; Gisbert, C. Bidding Zones of the European Power System: Benefits of a Multi-Dimensional Approach to the Evaluation of Possible Delineations. In Proceedings of the 2020 17th International Conference on the European Energy Market (EEM), Stockholm, Sweden, 16–18 September 2020; pp. 1–6.

12. Griffone, A.; Mazza, A.; Chicco, G. Applications of clustering techniques to the definition of the bidding zones. In Proceedings of the 2019 54th International Universities Power Engineering Conference (UPEC), Bucharest, Romania, 3–6 September 2019; pp. 1–6.

13. Consentec, F.E. *Relevance of Established National Bidding Areas for European Power Market Integration—An Approach to Welfare-Oriented Evaluation*; A report prepared for Bundesnetzagentur; Frontier: Frontier, UK, 2011. Available online: https://www.bundesnetzagentur.de/SharedDocs/Downloads/EN/Areas/ElectricityGas/Special%20Topics/StudyPriceZone/StudyPriceZoneLong.pdf?__blob=publicationFile&v=1 (accessed on 8 December 2023).

14. Burstedde, B. From nodal to zonal pricing: A bottom-up approach to the second-best. In Proceedings of the 2012 9th International Conference on the European Energy Market, Florence, Italy, 10–12 May 2012; pp. 1–8.

15. Imani, M.H.; Bompard, E.; Colella, P.; Huang, T. Forecasting electricity price in different time horizons: An application to the Italian electricity market. *IEEE Trans. Ind. Appl.* **2021**, *57*, 5726–5736. [CrossRef]

16. Breuer, C.; Seeger, N.; Moser, A. Determination of alternative bidding areas based on a full nodal pricing approach. In Proceedings of the 2013 IEEE Power & Energy Society General Meeting, Vancouver, BC, Canada, 21–25 July 2013; pp. 1–5.

17. Van den Bergh, K.; Wijsen, C.; Delarue, E.; D'haeseleer, W. The impact of bidding zone configurations on electricity market outcomes. In Proceedings of the 2016 IEEE International Energy Conference (ENERGYCON), Leuven, Belgium, 4–8 April 2016; pp. 1–6.

18. Trepper, K.; Bucksteeg, M.; Weber, C. Market splitting in Germany—New evidence from a three-stage numerical model of Europe. *Energy Policy* **2015**, *87*, 199–215. [CrossRef]

19. Egerer, J.; Weibezahn, J.; Hermann, H. Two price zones for the German electricity market—Market implications and distributional effects. *Energy Econ.* **2016**, *59*, 365–381. [CrossRef]

20. Plancke, G.; De Jonghe, C.; Belmans, R. The implications of two German price zones in a european-wide context. In Proceedings of the 2016 13th International Conference on the European Energy Market (EEM), Porto, Portugal, 6–9 June 2016; pp. 1–5.

21. Ilea, V.; Bovo, C. Impact of the price coupling of regions project on the day-ahead electricity market in Italy. In Proceedings of the 2017 IEEE Manchester PowerTech, Manchester, UK, 18–22 June 2017; pp. 1–6.

22. Grimm, V.; Martin, A.; Weibelzahl, M.; Zöttl, G. On the long run effects of market splitting: Why more price zones might decrease welfare. *Energy Policy* **2016**, *94*, 453–467. [CrossRef]

23. Grimm, V.; Martin, A.; Schmidt, M.; Weibelzahl, M.; Zöttl, G. Transmission and generation investment in electricity markets: The effects of market splitting and network fee regimes. *Eur. J. Oper. Res.* **2016**, *254*, 493–509. [CrossRef]

24. Ambrosius, M.; Grimm, V.; Kleinert, T.; Liers, F.; Schmidt, M.; Zöttl, G. Endogenous price zones and investment incentives in electricity markets: An application of multilevel optimization with graph partitioning. *Energy Econ.* **2020**, *92*, 104879. [CrossRef]

25. Fraunholz, C.; Hladik, D.; Keles, D.; Möst, D.; Fichtner, W. On the long-term efficiency of market splitting in Germany. *Energy Policy* **2021**, *149*, 111833. [CrossRef]

26. Weg, G. Economic Efficiency Analysis of Introducing Smaller Bidding Zones. 2015. Available online: https://www.eex.com/fileadmin/EEX/Downloads/Newsroom/Publications/Opinions_Expert_Reports/20150213-consentec-eex-bidding-zones-data.pdf (accessed on 21 October 2023).

27. ACER. *Report on the Influence of Existing Bidding Zones on Electricity Markets*; European Power Exchange: Paris, France, 2014.

28. Savelli, I.; Giannitrapani, A.; Paoletti, S.; Vicino, A. An optimization model for the electricity market clearing problem with uniform purchase price and zonal selling prices. *IEEE Trans. Power Syst.* **2017**, *33*, 2864–2873. [CrossRef]

29. Felder, F. Electricity Economics: Regulation and Deregulation. (Book Reviews). *Energy J.* **2003**, *24*, 151–153.

30. Kirschen, D.S.; Strbac, G. *Fundamentals of Power System Economics*; John Wiley & Sons: Hoboken, NJ, USA, 2018.

31. Lin, X.; Huang, T.; Liu, X.; Bompard, E.F.; Wang, B. A long-term congestion management framework through market zone configuration considering collusive bidding in joint spot markets. *IEEE Trans. Power Syst.* **2024**, 1–12. [CrossRef]

32. Lin, X.; Huang, T.; Wu, H.; Bompard, E.F.; Wang, B. Market zone configuration under collusive bidding among the conventional generators and renewable energy sources in the day-ahead electricity market. *Electr. Power Syst. Res.* **2024**, *232*, 110373. [CrossRef]

33. Jafari, M.; Bompard, E.; Delmastro, C.; Botterud, A.; Grosso, D. *Electrify Italy*; Enel Foundation: Torino, Italy, 2020.

34. Terna. Transparency Report: Installed Capacity. Available online: https://www.terna.it/en/electric-system/transparency-report/installed-capacity (accessed on 29 June 2023).
35. GME. About the Electricity Market—Introduction. Available online: https://www.mercatoelettrico.org/En/Mercati/MercatoElettrico/IlMercatoElettrico.aspx (accessed on 15 June 2023).
36. Terna. The New Electricity Market Zones: What You Need to Know. Available online: https://lightbox.terna.it/en/insight/new-electricity-market-zones (accessed on 15 June 2023).
37. Wu, H.; Solida, L.; Huang, T.; Bompard, E. Allowing Large Penetration of Concentrated RES in Europe and North Africa via a Hybrid HVAC-HVDC Grid. *Energies* **2023**, *16*, 3138. [CrossRef]
38. Terna. Publications: Monthly Report. Available online: https://www.terna.it/it/sistema-elettrico/pubblicazioni/rapporto-mesile (accessed on 20 September 2023).
39. Ardian, F.; Concettini, S.; Creti, A. Renewable generation and network congestion: An empirical analysis of the Italian power market. *Energy J.* **2018**, *39* (Suppl. S2), 3–40. [CrossRef]